Cyclodextrin Functionalized Graphene Nanosheets with High Supramolecular Recognition Capability: Synthesis and Host–Guest Inclusion for Enhanced Electrochemical Performance

Yujing Guo,[§,†,‡] Shaojun Guo,[§,†] Jiangtao Ren,[†] Yueming Zhai,[†] Shaojun Dong,[*,†] and Erkang Wang[*,†]

[†]State Key Laboratory of Electroanalytical Chemistry, Changchun Institute of Applied Chemistry, Chinese Academy of Sciences, Changchun 130022, Jilin, China, and Graduate School of the Chinese Academy of Sciences, Beijing, 100039, P. R. China, and [‡]Research Center for Environmental Science and Engineering, Shanxi University, Taiyuan, 030006, China. [§]Yujing Guo and Shaojun Guo contributed equally to this work.

ABSTRACT Cyclodextrins (CDs) are oligosaccharides composed of six, seven, or eight glucose units (α-, β-, or γ-CD, respectively), which are toroidal in shape with a hydrophobic inner cavity and a hydrophilic exterior. These interesting characteristics can enable them to bind selectively various organic, inorganic and biological guest molecules into their cavities to form stable host–guest inclusion complexes or nanostructured supramolecular assemblies in their hydrophobic cavity. On the other hand graphene nanosheet (GN), a rising-star material, holds great promise for potential applications in many technological fields due to its high surface areas, low cost, and high conductivity. If GNs are modified with CDs, it is possible to obtain new materials simultaneously possessing unique properties of GNs and cyclodextrins through combining their individual obvious advantages. In this article, we demonstrate for the first time a simple wet-chemical strategy for the preparation of CD–graphene organic–inorganic hybrid nanosheets (CD–GNs), which exhibited high solubility and stability in polar solvent. The obtained CD–GNs were characterized by UV–vis spectroscopy, static contact angle measurement, thermogravimetric analysis, X-ray photoelectron spectroscopy, Fourier transform infrared spectroscopy, Raman spectroscopy, atomic force microscopy, transmission electron microscopy, and electrochemical impedance spectroscopy, which confirmed that CD had been effectively functionalized on the surface of GNs. Furthermore, the formation mechanism of CD–GNs was also discussed. Interestingly, GNs here could load a number of CD molecules, which was very important for greatly enhancing the supramolecular function of CDs. Electrochemical results obviously reveal that CD–graphene organic–inorganic hybrid nanosheets could exhibit very high supramolecular recognition and enrichment capability and show much higher electrochemical response toward eight probe molecules (biomolecules and drugs) than unmodified GNs and carbon nanotubes, which is probably caused by the synergetic effects from GNs (high conductivity and high surface area) and CD molecules (host–guest recognition and enrichment).

KEYWORDS: graphene · cyclodextrin · supramolecular · electrochemical device · electrocatalysis

Graphene, a new two-dimensional (2D) structure consists of sp^2-hybridized carbon, is considered as a basic building block for graphitic materials of all other dimensionalities. As a "rising star" material, it has attracted considerable attention from both the experimental and theoretical scientific communities owing to its unique nanostructure and a variety of fascinating thermal, mechanical, and electrical properties.[1,2] This unique nanostructure also holds great promise for potential applications in many technological fields such as nanoelectronics,[3−6] nanophotonics,[7] nanocomposites,[8,9] sensors,[10,11] catalysis,[12] batteries,[13] and supercapacitors[14] because of its high surface areas (calculated value, 2630 m^2/g), potential low cost, and high conductivity. At present, graphene nanosheets (GNs) can mainly be prepared by three different techniques: (i) micromechanical cleavage, producing GNs in a very limited quantity, (ii) epitaxial growth of GN films on substrate, and (iii) chemical processing, involving graphite oxidation or ultrasonic or thermal exfoliation into graphene oxide (GO) and followed by the chemical reduction of GO. Among them, the wet-chemistry approach is the most suitable for the large scale production of GNs.[15,16] However, high-quality GNs with high hydrophobic property, unless well separated from each other, generally tend to form irreversible agglomerates or even restack to form graphite through strong π−π stacking interaction under certain strict conditions.[17] This problem has been initially resolved through large-scale production of GNs in the presence of a broad variety of protective reagents, including octadecylamine,[18] silicone,[19] polystyrene,[20] poly(sodium 4-styrenesulfonate),[21] 1-octyl-3-methylimidazolium,[22] DNA,[23] large aromatic molecules,[24] and didodecyldimethylammonium bromide,[25] *etc.* However, in most cases, the presence of dispersing

*Address correspondence to dongsj@ciac.jl.cn, ekwang@ciac.jl.cn.

Received for review April 30, 2010 and accepted June 18, 2010.

Published online June 28, 2010. 10.1021/nn100939n

agents in graphene composite may be undesirable for many technological applications, which usually lead to poor performance.[26] Therefore, designing or introducing a new functional molecules for effectively dispersing GNs and meanwhile bringing in new or enhanced functions is highly desirable and technologically important.

CDs are oligosaccharides composed of six, seven, or eight glucose units (α, β, or γ-CD, respectively), which are toroidal in shape with a hydrophobic inner cavity and a hydrophilic exterior. The interesting characteristics can enable them to bind selectively various organic, inorganic, and biological guest molecules into their cavities to form stable host−guest inclusion complexes or nanostructured supramolecular assemblies in their hydrophobic cavity, showing high molecular selectivity and enantioselectivity.[27−29] Particularly, the selective association of target molecules to the hydrophobic cavities of CDs (The binding constants of target molecules with β-CD are generally strong and more than 10^3) has been used to develop different sensors and separation matrices based on the strong recognition and enrichment functions of CDs.[27−29] And also, CDs are environmentally friendly, water-soluble, and can improve the solubility and stability of functional materials. If GNs are modified with CDs, it is possible to obtain new materials simultaneously possessing the unique properties of GNs (large surface area and high conductivity) and CDs (high supramolecular recognition and enrichment capability) through combining their individual characteristics, which will provide good opportunities for applications in the fields of sensors, electrocatalysis, luminescence, and electronics, *etc*.[30]

In this article, we demonstrate for the first time the use of CD in the preparation of stable (exceed 6 months) aqueous suspension of GNs with concentrations over 2.5 mg/mL *via* a simple wet-chemical strategy. UV−vis spectroscopy, static contact angle measurement, thermogravimetric analysis (TGA), X-ray photo-electron spectroscopy (XPS), Fourier transform infrared (FTIR), Raman spectroscopy, atomic force microscopy (AFM), transmission electron microscopy (TEM), and electrochemical impedance spectroscopy (EIS) were used to characterize the structure and composition of CD−graphene organic−inorganic hybrid nanosheets. TGA data reveal that GNs here could load a number of CD molecules (carbon nanotubes can only load a small fraction of CD molecules), which was very important for greatly enhancing the supramolecular function of CD−GNs due to the presence of many CD molecules on the surface of the GNs. Specially, the results from electrochemistry obviously reveal that CD−graphene hybrid nanosheets could exhibit very high supramolecular recognition and enrichment capability and show much higher electrochemical performance toward eight probe molecules (biomolecules and drugs) than unmodified GNs and carbon nanotubes (CNTs), which is probably caused by the synergetic effects from GNs (high conductivity and high surface area) and CDs (host−guest recognition and enrichment).

RESULTS AND DISCUSSION

Generally, GO can form a stable dispersion in water because of its high oxygen-containing groups. However, if the oxygen functionality was removed by chemical reduction to yield graphene, GNs would immediately lose their water dispersibility, then aggregate, and eventually precipitate due to the prominent interlayer π−π conjugate interaction of GNs.[2] To overcome this, we judiciously introduced CD molecules into GO before it was fully reduced, and the resulted GNs remain soluble in water and do not aggregate for a long time. Scheme 1 shows the procedure for preparing CD-graphene organic−inorganic hybrid nanosheets and GNs, and sensing the guest molecules by an electrochemical strategy. In a typical synthesis of a CD−GN hybrid nanosheet, the homogeneous GO dispersion was mixed with CD aqueous solution, ammonia, and hydrazine solution. After being stirred for a few minutes and kept at 60 °C water bath for more than 3.5 h, the stable black dispersion of CD−GNs was obtained (Figure 1B, label b).

UV−vis spectroscopy was used to monitor the reaction process for the formation of very stable β-CD−GNs dispersion (Note that here β-CD was employed as a model in the following characteristic and electrochemical experiments except for the specified statement). As shown in Figure 1A, the GO dispersion displays an maximum absorption at 231 nm which is due to the π−π* transition of aromatic C═C bonds and a shoulder at ∼290−300 nm which corresponds to the n−π* transition of the C═O bond.[31] With the increase of the reaction time, the colors of the dispersion change from pale-yellow (Figure 1B, label a) to dark-brown, and finally black (Figure 1B, label b). The absorption peak of the GO dispersion at 231 nm gradually shifts to 264 nm, and the absorbance in the whole spectral region increases, suggesting that the electronic conjugation within the GNs is restored upon the reduction by hydrazine.[32] Little increase in absorbance is found after 3.5 h, indicating the completion of reduction reaction within that period. Particularly, the dispersion is stable and no obvious precipitates are observed after being stored for more than 6 months (Figure 1B, label b). α,γ-CD molecules were also used as protecting agents for preparing stable CD−GNs suspension, and their corresponding results are shown in Supporting Information, Figure S1. It is found that α,γ-CD−GNs still exhibited excellent stability even after being stored for more than 6 months. In contrast, the reduction of GO dispersion without any stabilizer led to the precipitation of GNs after being stored for less than 2 weeks (Figure 1B, label c), due to their irreversible aggregation. The static contact angle measurements were performed to investigate the hy-

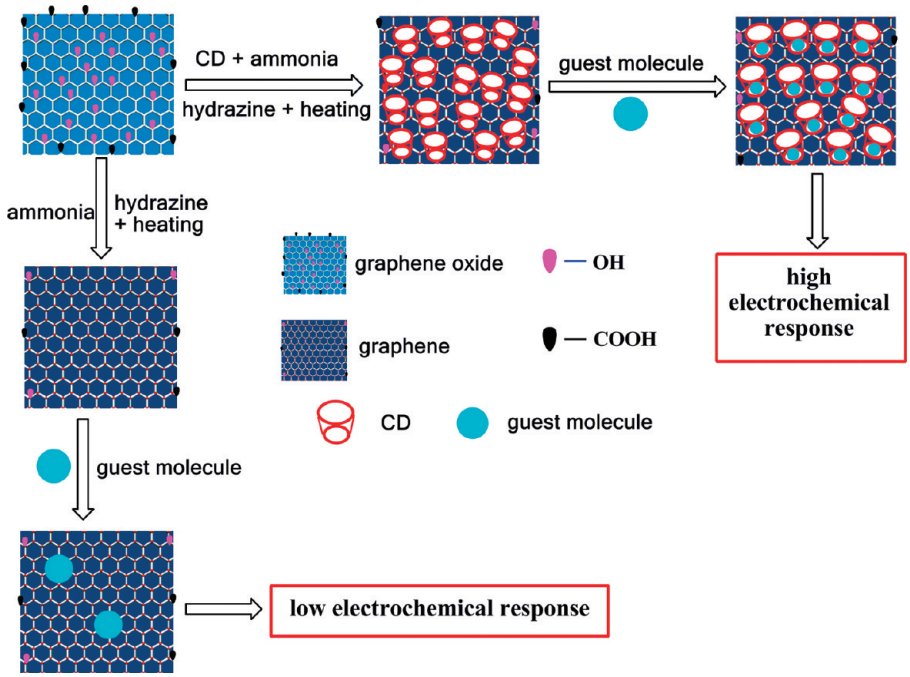

Scheme 1. Illustration of the procedure for preparing CD−graphene organic−inorganic hybrid nanosheets and GNs, and sensing the guest molecules by an electrochemical strategy.

drophilic/hydrophobic features of GNs and CD−GNs. It is noted that the unmodified GNs have a relatively hydrophobic interface with a contact angle of about 81.2° (Figure 1C). Whereas the interface of CD−GNs is much more hydrophilic with a contact angle of 38.3° (Figure 1D). These results indicate that the reduced GNs were protected by CD molecules. TGA was further used to determine the amount of CD molecules on the surface of GNs. Figure 2A displays the weight losses of CDs (curve a) and CD−GNs (curve b). It is found that the weight-loss region (about 280 °C) could be attributed to the decomposition of CDs. The significant weight reduction in the high-temperature region (about 590 °C) was due to the decomposition of GNs. Thus, the amount of CD molecules was determined to be 38.2 wt % (about one CD per 152 carbon atoms), indicating that a number of CD molecules could be adsorbed on the surface of GNs. This is an amazing result because GNs loading so many CD molecules will have a good opportunity to develop the supramolecular recognition and enrichment ability

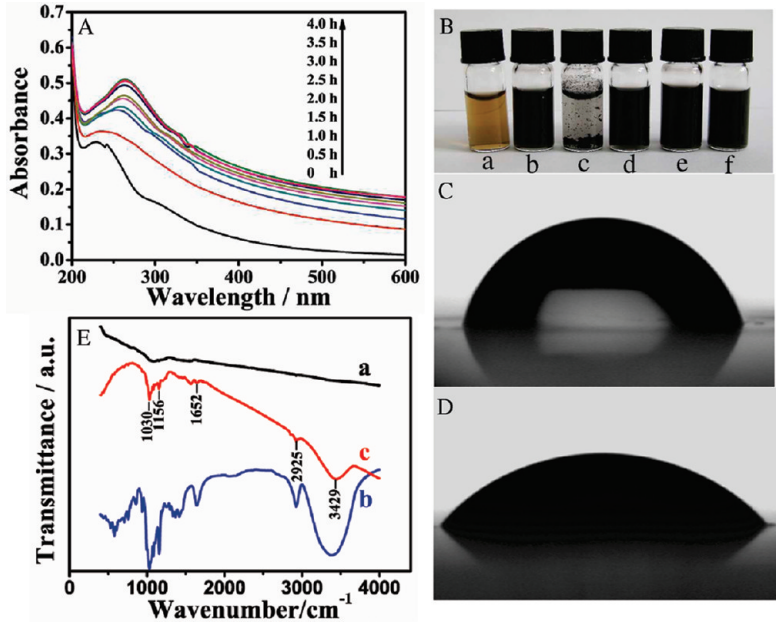

Figure 1. (A) UV−vis absorption spectra of GO dispersions during the reaction period (4 h). (B) Photographs of GO (a), CD−GNs (b), and GNs (c) dispersions in water; CD−GNs dispersion in alcohol (d), DMF (e), and DMSO (f). (C, D) The shape of a water droplet on the surface of GNs (C) and CD−GNs (D). (E) FT-IR spectra of GNs (a), CD (b), and CD−GNs (c).

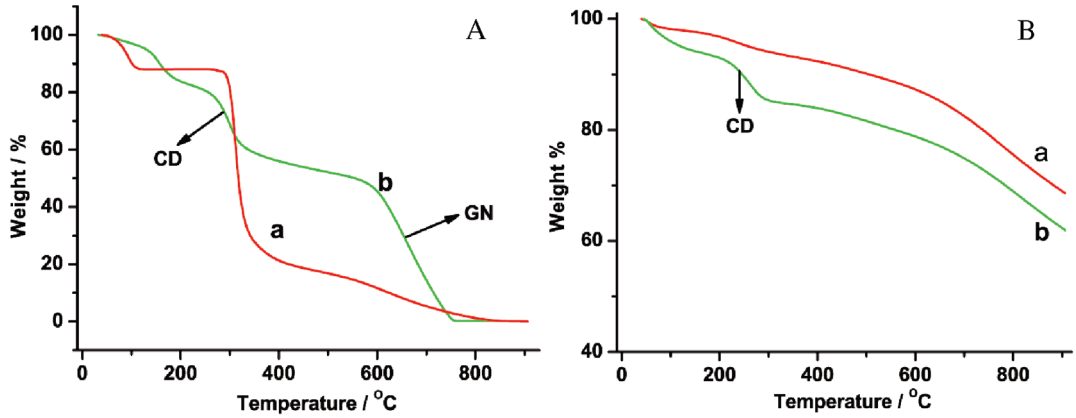

Figure 2. (A) TGA of CD (curve a) and CD−GNs (curve b); (B) TGA of CNTs (curve a) and CD−CNTs (curve b).

of CDs (the following electrochemical data will reveal this point). As a comparison, the TGA of CNTs (curve a) and CD-CNTs (curve b) has also been investigated, as shown in Figure 2B. It is found that COOH-functionalized CNTs can only load a small fraction of CD molecules (about 9.5 wt %). FT-IR spectra of CD, CD−GNs, and unmodified GNs are shown in Figure 1E. It is found that the FT-IR spectrum of GNs (curve a) is essentially featureless except the C═C conjugation (1550 cm^{-1}) and C−C band (1190 cm^{-1}), *etc.* Whereas the FT-IR spectrum of CD−GNs (curve c) exhibits typical CD absorption features (curve b) of the ring vibrations at 578, 708, 756, and 943 cm^{-1}, the coupled C−O−C stretching/O−H bending vibrations at 1156 cm^{-1}, the coupled C−O/C−C stretching/O−H bending vibrations at 1030 and 1079 cm^{-1}, CH_2 stretching vibrations at 2925 cm^{-1}, C−H/O−H bending vibrations at 1416 cm^{-1}, and O−H stretching vibrations at 3429 cm^{-1}. This clearly confirms that CD molecules are attached to the surface of GNs. According to the previous report,[33−37] multiple hydrogen bondings could be strong enough to construct a complex structure. For instance, hydrogen bonding could be used as a driving force to construct layer-by-layer (LBL) assembling film.[33−37] Furthermore, from the understanding of the molecular level, the O−H stretching vibration peak could exhibit typical red-shift when hydrogen bonding is formed.[33] Note that the O−H stretching vibration peak at 3429 cm^{-1} for CD−GNs (bonded OH mode) exhibits typical large red-shift relative to free OH mode (located at about 3700 cm^{-1}),[33] indicating that there exists a strong hydrogen bond between CD molecules and some oxygen-containing groups of GNs.[33] To further clarify the interaction mechanism between CD and GNs, we employed some sugars (glucose, fructose, and sucrose), which have similar structures with CDs (all of them contain some −OH groups), as protecting agents for synthesizing GNs. It is found that the GNs protected by sugar still exhibited high solubility and stability, as shown in Supporting Information, Figure S2. Considering the molecular structure of GN and CDs, there only possibly exist two molecular interactions: hydrophobic and hydrogen-bonding interactions. Owing to the hydrophobic cavity of CD molecules located inside and GNs themselves being of micrometer size, the hydrophobic interaction between CD and GNs is impossible. Since CD and GNs (derived from GO) contain multiple OH groups, the formation of strong hydrogen bondings between them is strongly supported, which is in accordance with the above experimental facts and IR data. On the basis of these facts, the mechanism for specific adsorption of CDs on GNs was considered as follow: Generally, GOs have many oxygen-containing groups, particularly an −OH group.[32] When CDs were added into GO solution, they would be adsorbed on the surface of GO because of the strong hydrogen bondings between them (the corresponding solution exhibited very high stability, data not shown). Then, the strong reducing agent (hydrazine) consisting mostly of oxygen-containing groups would be reduced to produce the GNs. The remaining oxygen-containing groups, particularly the −OH group (generally, the GNs produced *via* the chemical reduction method have some oxygen-containing groups[2,32]), had to continue to form the strong hydrogen bonding with the CDs, possessing a number of −OH groups on both conical faces for stabilizing the GNs. Thus, the CD molecules were covered on the surface of GNs and could prevent their coalescence and aggregation. However, the detailed interaction mechanism between GN and CDs is not very clear at present and needs further study. Furthermore, CD−GNs could disperse well into other organic solvents such as ethanol, dimethylformamide (DMF), and dimethylsulfoxide (DMSO) (Figure 1B, label d−f). This may extend the use of the new material.

To further illustrate the formation of GNs, XPS was performed to characterize the removal of the oxygen groups. Figure 3A shows the C1s deconvolution spectrum of GO, revealing the presence of four types of carbon bonds: C−C (284.6 eV), C−O (286.7 eV), C═O (287.8 eV), and O−C═O (288.7 eV).[38,39] After GO was reduced to CD−GNs, the corresponding XPS spectrum (Figure 3B) shows that the intensity of the peaks associated with C−C (284.6 eV) became predominant, while

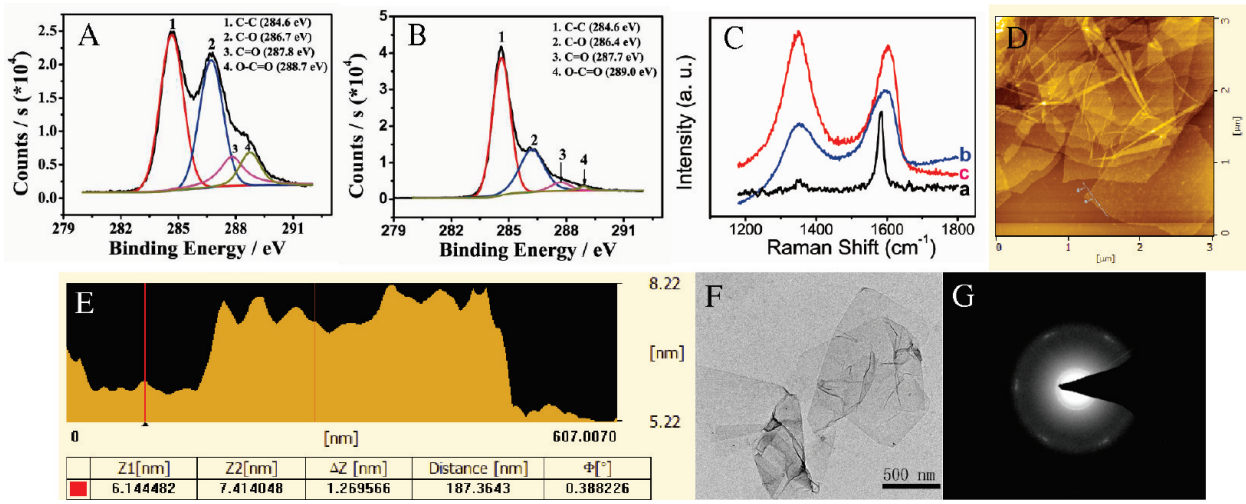

Figure 3. The deconvolution of C1s spectra of GO (A) and CD−GNs (B). (C) Raman spectra of graphite (a), GO (b), and CD−GNs (c). (D) AFM image of CD−GNs. (E) The cross section identified by the line in Figure 4D shows the height of CD−GNs. TEM (F) and ED (G) images of CD−GNs.

the intensities of all C1s peaks of the carbon binding to oxygen, especially the peak of C−O (epoxy and alkoxy), decreased dramatically, indicating that most of the oxygen-containing functional groups were removed after the reduction. Raman spectroscopy is one of the most widely used techniques to characterize the structural and electronic properties of graphene including disorder and defect structures, defect density, and doping levels. G band is usually assigned to the E_{2g} phonon of C sp^2 atoms (usually observed at ~1575 cm^{-1}), while D band is a breathing mode of κ-point phonons of A_{1g} symmetry (~1350 cm^{-1}).[40] Figure 3C shows the Raman spectrum of pristine graphite (curve a), GO (curve b), and CD−GNs (curve c). Raman spectrum of the pristine graphite displays a strong G band at 1583 cm^{-1} and a very weak D band at 1352 cm^{-1}, whereas for the Raman spectroscopy of GO and CD−GNs, the G band is broadened and shift upward to more than 1595 cm^{-1}, which was mainly caused by stress. Note that the D band at 1352 cm^{-1} increases substantially, indicating the reduction in size of the in-plane sp^2 domains, possibly due to the extensive oxidation and ultrasonic exfoliation. When GO was chemically reduced to CD−GNs, the Raman spectrum of CD−GNs also contained both G and D bands (at 1598 and 1352 cm^{-1}, respectively), but exhibited a slightly increased D/G intensity ratio relatively to that of GO. This change may suggest a decrease in the average size of the sp^2 domains from CD−GNs and a partially ordered crystal structure of the CD−GNs, which can be well explained by the creation of numerous new graphitic domains in CD−GNs that are smaller in size than the ones presented in GO.[41,42]

Figure 3D shows the AFM image of CD−GNs. A number of flake-like nanostructures are obviously found, revealing the feasibility of the present strategy. The corresponding cross-sectional view, as shown in Figure 3E, indicates that the average thickness of CD−GNs was about 1−2 nm, which is a typical characteristic of functional-molecule-protected single-layer graphene.[1] The greater thickness of CD−GNs than that of GO could be attributed to the CD molecules grafted onto both sides of GNs. TEM imaging (Figure 3F) and electron diffraction (ED, Figure 3G) were further used to characterize the CD−GNs. The TEM image of CD−GNs illustrates the flake-like shapes of graphene. Particularly, some distortions caused by the extreme lack of thickness of the CD−GNs lead to a wrinkled topology. The ED pattern of our CD−GNs is similar to those of peeled-off GNs,[41,42] suggesting a well-crystallized graphene structure.

As is known, in electrochemical impedance spectrum, the semicircle portion observed at high frequencies corresponds to the charge transfer limiting process.[41] The charge transfer resistance (R_{ct}) can be directly measured as the semicircle diameter. As we can see from Figure 4, when GO was modified onto the glassy carbon (GC) electrode, the semicircle dramatically increases (curve c) relative to the bare GC elec-

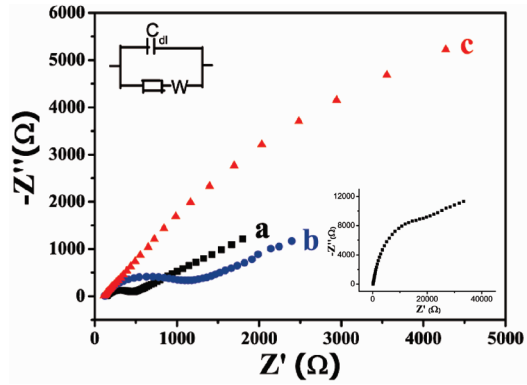

Figure 4. EIS plots of bare GC (curve a), CD−GNs/GC (curve b), and GO/GC electrodes (curve c). EIS experiments were conducted in 0.1 M KCl solution containing 2.5 mM $K_3Fe(CN)_6$ and 2.5 mM $K_4Fe(CN)_6$. The inset (bottom-right corner) shows the whole EIS plot of the GO/GC electrode.

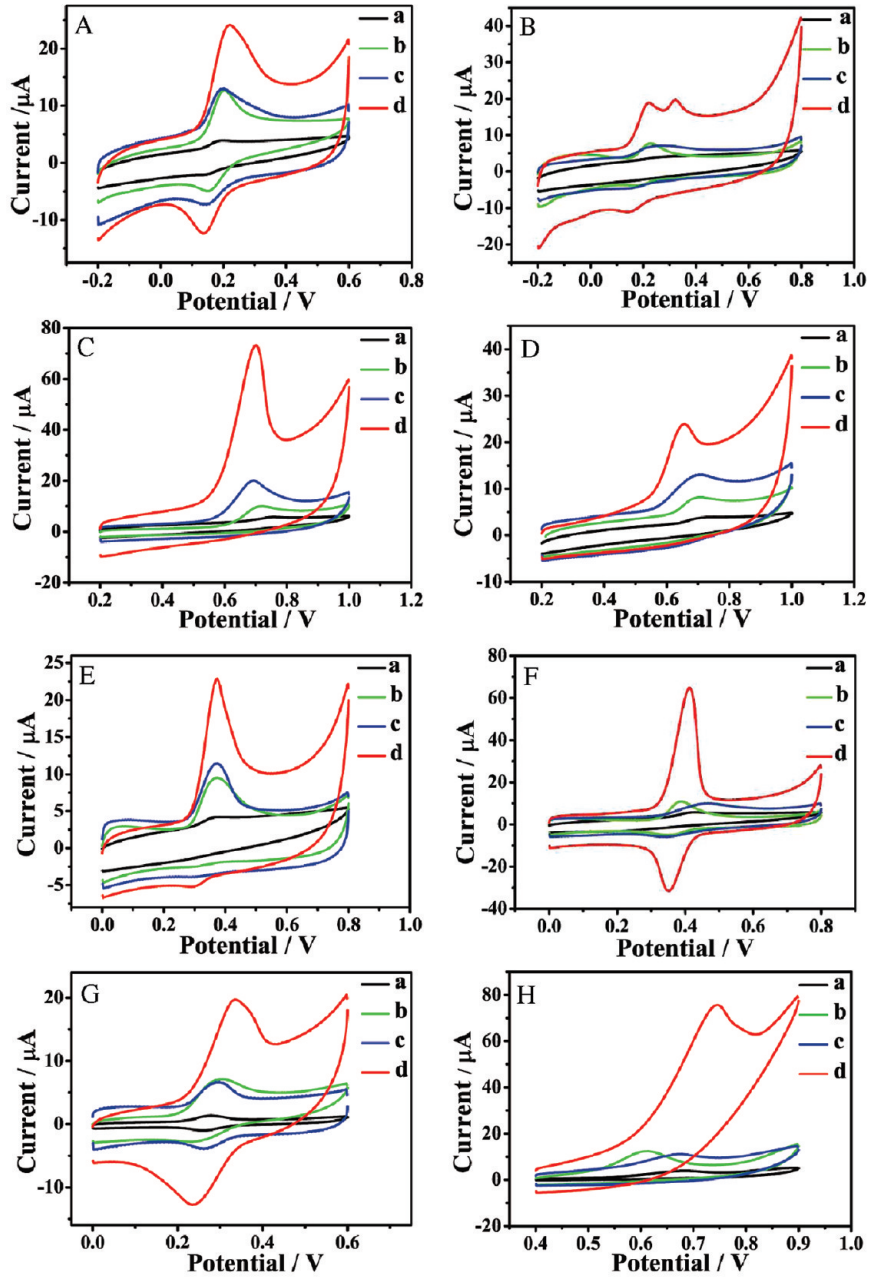

Figure 5. CVs of 50 μM DA (A), NP (B), Trp (C), Tyr (D), UA (E), APAP (F), rutin (G), and thioridazine (H) at GC electrode (curve a), CNTs/GC (curve b), GNs/GC electrode (curve c), and CD−GNs/GC electrode (curve d) in 0.1 M phosphate buffer (pH 7.4). Scan rate: 50 mV s^{-1}.

trode (curve a), suggesting that GO acted as an insulating layer which made the interfacial charge transfer difficult. After CD−GNs were modified on the surface of the GC electrode (curve b), the semicircle decreased distinctively, indicating that CD−GNs could accelerate the electron transfer between the electrochemical probe $[Fe(CN)_6]^{3-/4-}$ and the GC electrode, which is attributed to the significantly improved electrical conductivity of CD−GNs films. In addition, as shown in Supporting Information, Figure S3 (SEM image), CD−GNs could form a homogeneous film when modified on a GC electrode interface. These important characteristics enable CD−GNs to be a good material for electrochemical sensing and biosensing. It should be noted here that introducing a number of CDs onto the surface of GNs cannot only improve the stability and dispersion of graphene, but also be expected to enhance the sensitivity of detection for some important biomolecules and drugs through the formation of supramolecular complexes between CDs and the guest molecules. To demonstrate this concept (Scheme 1), the electrochemical behaviors of five kinds of electroactive biomolecules [dopamine (DA), uric acid (UA), norepinephrine (NP), tyrosine (Tyr), and tryptophan (Trp)] and three kinds of drugs [acetaminophen (APAP), rutin, and thioridazine], which can form inclusion complexes with

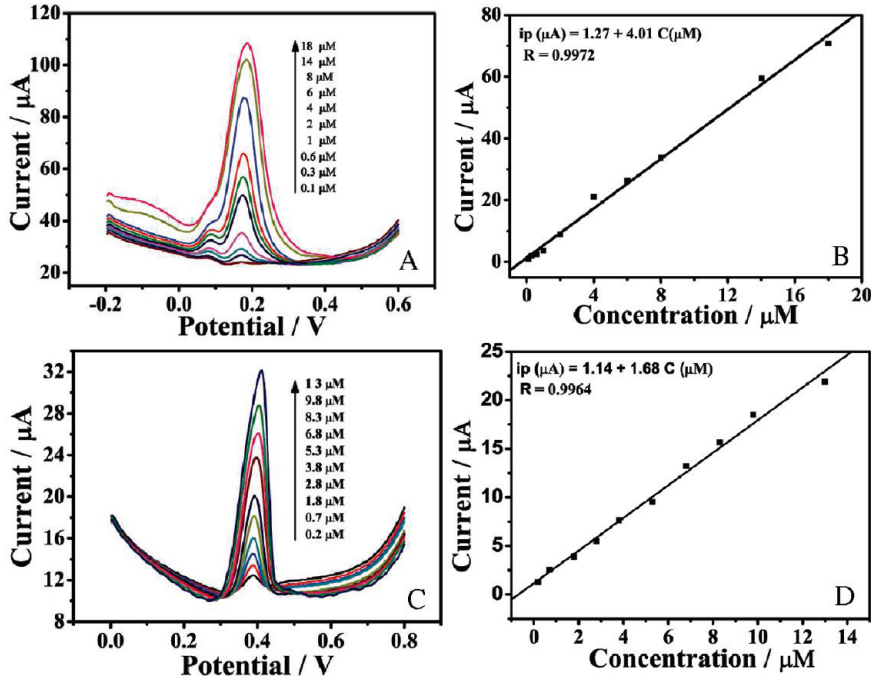

Figure 6. (A) The differential pulse voltammetric (DPV) response for the different concentrations of DA at CD−GNs/GC electrode in 0.1 M phosphate buffer (pH 7.4): pulse period, 0.2 s; amplitude, 50 mV. (B) The calibration curve of DA. (C) DPV response for the different concentrations of APAP at CD−GNs/GC electrode in 0.1 M phosphate buffer (pH 7.4): pulse period, 0.2 s; amplitude, 50 mV. (D) The calibration curve of APAP.

β-CD, were investigated. Figure 5 shows cyclic voltammograms (CVs) of the above eight compounds at GC (curve a), CNTs/GC (curve b), GNs/GC (curve c), and CD−GNs/GC (curve d) electrodes. All the oxidation peak currents of eight compounds are increased at CNTs/GC and GNs/GC electrodes relative to the currents at the bare GC electrode, indicating a favorable catalytic activity of GNs and CNTs toward the oxidation of the compounds. While at the CD−GNs/GC electrode, all show a remarkable increase in the peak currents relative to that at the other three electrodes. This illustrates that β-CD molecules on the surface of GNs with high supramolecular recognition capability can form inclusion complexes with all the investigated analytes. The inclusion action can further enhance the accumulation effect of CD−GNs/GC electrode and accordingly increase the concentration of analytes on the interface of the modified electrode, which leads to pronounced peak current increased. These phenomena suggest that the CD−GNs not only show the excellent properties of GNs but also exhibit the excellent supramolecular recognition capability of CDs. The greatly enhanced electrochemical reactivity of the above compounds at the CD−GNs/GC electrode relative to the reactivity of those at the other three electrodes makes the CD−GNs/GC electrode a better choice for the electrochemical sensing of the above compounds at physiological pH.

As introduced above, the enrichment effect of CDs is very important for obviously improving the electrochemical performance for target molecules. However, it is hard for CDs themselves to complete the task because CDs are easily detached from the surface of an electrode when they are modified on the electrode, and particularly CDs themselves have poor conductivity. Therefore, a CD-modified interface will not have a good opportunity to develop a high supramolecular recognition and enrichment ability toward target molecules. CNT−CD hybrids can effectively enhance the conductivity of CD molecules. However, CNTs themselves (even CNTs with as many COOH groups as possible) could only immobilize a few CD molecules (determined from the above TGA data). Thus, the CNT−CD hybrids will not well embody the recognition and enrichment functions of CDs. But, we found that GNs derived from GO could load a number of CD molecules (up to 38.2 wt %). This is an amazing result, which could be understood from the following. (a) A number of CDs supported on the surface of GNs can develop their supramolecular recognition and enrichment functions more effectively, exhibiting much higher electrochemical performance than individual GN and CNT (shown in Figure 5). (b) GNs as a support can enhance the electron transfer from target molecules (enriched into CDs, the binding constants of target molecules with β-CD are generally more than 10^3) to electrode in addition to their providing high surface area for loading CDs. (c) GN−CDs hybrids exhibited high stability and solubility in water. When they were modified on the electrode, GN−CDs could form a homogeneous film (shown in Supporting Information, Figure S3), which facilitated the construction of reproducible electrochemical sensors with high-sensitivity.

To demonstrate the sensing performance of CD−GNs toward certain substances, two model molecules (DA, a neurotransmitter that affects the brain processes that control movement, emotional response, and the capacity to feel pleasure and pain; APAP, being one of the most extensively employed drugs in the world, is a noncarcinogenic drug and an effective substitute for aspirin) were chosen as a representative analyte of biomolecules and drugs, respectively. Figure 6 panels A and B illustrate the differential pulse voltammetric (DPV) response for different concentrations of DA (Figure 6A) and APAP (Figure 6B), respectively. The current response for the oxidation (i_{pa}) process is directly proportional to the analyte concentration within 0.1−18 μM and 0.2−13 μM for DA and APAP, respectively, and, the detection limits were 20 and 40 nM for DA and APAP, respectively, which are more sensitive than those of carbon nanotube (CNT)-β-CD modified GC electrode (37 μM for DA)[43] and polyaniline-CNT composite electrode (0.25 μM for APAP), *etc.*[44] Also, the CD−GNs/GC electrode shows the high current densities of 6.93, 6.51, 18.7, and 5.63 mA mM^{-1} L cm^{-2} for DA, UA, APAP, and rutin, respectively, which is much higher than those of recent state-of-art nanomaterials, such as chemically reduced graphene oxide (about 0.278, 0.368, 0.377 mA mM^{-1} L cm^{-2} for DA, UA, and APAP, respectively),[45] CNTs/quercetin/Nafion composite film (about 0.122 mA mM^{-1} L cm^{-2} for DA),[46] and CD/CNTs composite film (about 0.063 mA mM^{-1} L cm^{-2} for rutin),[47] *etc*. These comparison data further indicate that the CD−GNs/GC electrode exhibits very high electrochemical performance toward the target molecules. Therefore, we think that this simple and reliable strategy based on an electrochemical technique at the CD−GNs/GC electrode could be probably applied to the development of sensitive electrochemical sensors to determine a wide variety of organic or inorganic electroactive compounds.

CONCLUSIONS

A simple and fast method was successfully developed to obtain CD−graphene organic−inorganic hybrid nanosheets, which exhibit high solubility and stability in water, ethanol, DMF, and DMSO. Most importantly, we verified that a few biological and drug properties of interest (can form stable host−guest inclusion complexes with CDs) at the CD−GN/GC electrode exhibited much higher electrochemical performance than those of CNTs/GC, GNs/GC, and bare GC electrodes, revealing that the CD−GNs not only show the good electrical and large-surface-area properties of GNs but also exhibit high supramolecular recognition and enrichment properties of CDs. We believe the introduction of a great number of CDs into graphene will probably bring important applications in various fields because of the tunable cavity size of different kinds of CDs.

EXPERIMENTAL SECTION

Materials. Graphite was purchased from Alfa Aesar. β-CD, glucose, fructose, sucrose, UA, DA, NP, Tyr, Trp, APAP, rutin, hydrazine solution (50 wt %), and ammonia solution (25−28 wt %) were obtained from Beijing Chemical Reagent factory (Beijing, China). α,γ-CDs and thioridazine were obtained from Sigma. Carbon nanotubes (CNTs) (Shenzhen Nanotech Port Co., Ltd.) with a diameter of 20−50 nm were obtained through the CVD method and purified with 2.6 M HNO_3 at 120 °C for 24 h. Then, the purified CNTs were treated with a 1:3 v/v mixture of HNO_3 (65%) and H_2SO_4 (98%) at room temperature for 8 h with continuous ultrasonication. The product was centrifuged, washed with ethanol, and dried under vacuum at 60 °C overnight. The resulting COOH-functionalized CNTs can be easily dissolved in water. Other chemicals were of analytical grade and used without further purification. Water used throughout all experiments was purified with the Millipore system.

Apparatus. A XL30 ESEM scanning electron microscope was used to determine the morphology of CD−GNs modified electrode. TEM images were obtained with a TECNAI G_2 high-resolution transmission electron microscope operating at 200 kV. AFM image was taken by using a SPI3800N microscope (Seiko Instruments Industry Co., Tokyo, Japan) (Seiko Instruments, Inc.) operating in the tapping mode with standard silicon nitride tips. Typically, the surface was scanned at 1 Hz with the resolution of 256 lines/image. FTIR was recorded on a Bruker Vertex 70 spectrometer (2 cm^{-1}). TGA was carried out by using a Perkin-Elmer TGA-2 thermogravimetric analyzer at a heating rate of 10 °C min^{-1} under vacuum from 40 to 900 °C. XPS measurement was performed on an ESCALAB-MKII 250 photoelectron spectrometer (VG Co.) with Al Kα X-ray radiation as the X-ray source for excitation. The sample for XPS characterization was dropped on a Cu substrate. UV−vis absorption spectra were recorded on a Cary 500 UV−vis−NIR spectrometer (Varian, U.S.A.). Raman spectra were recorded with a Renishaw 2000 equipped by an Ar^+ ion laser giving the excitation line of 514.5 nm and an air-cooling charge-coupled device (CCD) as the detector (Renishaw Co., U.K.). Contact angles were measured on a drop shape analysis system G10/DSA10 contact angle system. Electrochemical measurements were carried out on CHI832B electrochemical workstation (ChenHua Instruments Co., Shanghai, China). A three-electrode system was used in the experiment with a bare and the modified GC electrode (3 mm in diameter) as the working electrode, respectively. An Ag/AgCl electrode (saturated KCl) and a Pt wire electrode were used as reference electrode and counter-electrode, respectively. The electrochemical impedance measurements were carried out with an Autolab/PG30 electrochemical analyzer system (ECO Chemie B. V. Netherlands) in a grounded Faraday cage at ambient temperature. The interfacial charge-transfer resistances for different modified surface were determined by EIS in the frequency range between 0.1 Hz and 1 MHz with a perturbation signal of 5 mV.

Synthesis of CD−graphene Organic−inorganic Hybrid Nanosheets and Pure Graphene. GO nanosheets were synthesized from natural graphite by a modified Hummers' method.[48,49] A CD−graphene hybrid nanosheet was prepared as follows: A 20.0 mL portion of the homogeneous graphene oxide dispersion (0.5 mg/mL) was mixed with 20.0 mL of 80 mg/mL α-, β-, or γ-CD aqueous solution and 300.0 μL of ammonia solution, followed by the addition of 20 μL of hydrazine solution. After being vigorously shaken or stirred for a few minutes, the vial was put in a water bath (60 °C) for 3.5 h. The stable black dispersion was obtained. The dispersion was filtered with a nylon membrane (0.22 μm) to obtain CD−graphene organic−inorganic hybrid nanosheets that can be redispersed readily in water (0.25 mg/mL) by ultrasonication. Additionally, the preparation of pure graphene was similar with

CD−graphene organic−inorganic hybrid nanosheets except there was no addition of CD.

Synthesis of CDs/CNTs Nanocomposite. A 25 mg portion of COOH-functionalized CNTs was dissolved in 50 mL of water, followed by the addition of 200 mg of β-CD. Then, the mixture was stirred for more than 12 h. After centrifugation for four times with water, the product was dried under vacuum at 60 °C overnight.

Preparation of Graphene, CNT, and CD-Graphene Modified Electrode. Prior to modification, the GC electrode was polished with 1, 0.3, and 0.05 μm alumina slurry, rinsed thoroughly with doubly distilled water between each polishing step, then washed successively with 1:1 nitric acid, acetone, and doubly distilled water in an ultrasonic bath and dried in air. The GNs/GC, CNTs/GC, and CD−GNs/GC electrodes were obtained by casting 5 μL of 0.25 mg/mL GNs or CNTs or CD−GNs suspension on the surface of a well-polished GC electrode and dried in air. Finally, the modified electrodes were activated by several successive scans with a scan rate of 50 mV/s in phosphate buffer solution (pH 7.4) until a steady voltammogram was obtained.

Acknowledgment. This research was supported by the National Natural Science Foundation of China (Nos. 20735003, 20890020, and 20820102037) and 973 Project (Nos. 2009CB930100 and 2010CB933600) and the China Postdoctoral Science Foundation (No. 20090451143).

Supporting Information Available: Photographs of CD−GNs dispersion in water; SEM images of CD−GNs modified GC electrode at different magnifications. This material is available free of charge *via* the Internet at http://pubs.acs.org.

REFERENCES AND NOTES

1. Rao, C. N. R.; Sood, A. K.; Subrahmanyam, K. S.; Govindaraj, A. Graphene: The New Two-Dimensional Nanomaterial. *Angew. Chem., Int. Ed.* **2009**, *48*, 7752–7777.
2. Xu, Y. X.; Bai, H.; Lu, G. W.; Li, C.; Shi, G. Q. Flexible Graphene Films *via* the Filtration of Water-Soluble Noncovalent Functionalized Graphene Sheets. *J. Am. Chem. Soc.* **2008**, *130*, 5856–5857.
3. Li, X. L.; Wang, X. R.; Zhang, L.; Lee, S.; Dai, H. J. Chemically Derived, Ultrasmooth Graphene Nanoribbon Semiconductors. *Science* **2008**, *319*, 1229–1232.
4. Pang, S. P.; Tsao, H. N.; Feng, X. L.; Müllen, K. Patterned Graphene Electrodes from Solution-Processed Graphite Oxide Films for Organic Field-Effect Transistors. *Adv. Mater.* **2009**, *21*, 3488–3491.
5. Wu, Z.-S.; Pei, S. F.; Ren, W. C.; Tang, D. M.; Gao, L. B.; Liu, B. L.; Li, F.; Liu, C.; Cheng, H.-M. Field Emission of Single-Layer Graphene Films Prepared by Electrophoretic Deposition. *Adv. Mater.* **2009**, *21*, 1756–1760.
6. Di, C.- A.; Wei, D. C.; Yu, G.; Liu, Y. Q.; Guo, Y. L.; Zhu, D. B. Patterned Graphene as Source/Drain Electrodes for Bottom-Contact Organic Field-Effect Transistors. *Adv. Mater.* **2008**, *20*, 3289–3293.
7. Xu, Y. F.; Liu, Z. B.; Zhang, X. L.; Wang, Y.; Tian, J. G.; Huang, Y.; Ma, Y. F.; Zhang, X. Y.; Chen, Y. S. A Graphene Hybrid Material Covalently Functionalized with Porphyrin: Synthesis and Optical Limiting Property. *Adv. Mater.* **2009**, *21*, 1275–1279.
8. Pasricha, R.; Gupta, S.; Srivastava, A. K. A Facile and Novel Synthesis of Ag−Graphene-Based Nanocomposites. *Small* **2009**, *5*, 2253–2259.
9. Vickery, J. L.; Patil, A. J.; Mann, S. Fabrication of Graphene−Polymer Nanocomposites with Higher-Order Three-Dimensional Architectures. *Adv. Mater.* **2009**, *21*, 2180–2184.
10. Lu, C.-H.; Yang, H.-H.; Zhu, C.-L.; Chen, X.; Chen, G.-N. A Graphene Platform for Sensing Biomolecules. *Angew. Chem., Int. Ed.* **2009**, *48*, 4785–4787.
11. Lu, J.; Do, I.; Drzal, L. T.; Worden, R. M.; Lee, I. Nanometal-Decorated Exfoliated Graphite Nanoplatelet Based Glucose Biosensors with High Sensitivity and Fast Response. *ACS Nano* **2008**, *2*, 1825–1832.
12. Seger, B.; Kamat, P. V. Electrocatalytically Active Graphene−Platinum Nanocomposites. Role of 2-D Carbon Support in PEM Fuel Cells. *J. Phys. Chem. C.* **2009**, *113*, 7990–7995.
13. Wang, D. H.; Choi, D.; Li, J.; Yang, Z. G.; Nie, Z. M.; Kou, R.; Hu, D. H.; Wang, C. M.; Saraf, L. V.; Zhang, J.; Aksay, I. A.; Liu, J. Self-Assembled TiO_2-Graphene Hybrid Nanostructures for Enhanced Li-Ion Insertion. *ACS Nano* **2009**, *3*, 907–914.
14. Tang, L. H.; Wang, Y.; Li, Y. M.; Feng, H. B.; Lu, J.; Li, J. H. Preparation, Structure, and Electrochemical Properties of Reduced Graphene Sheet Films. *Adv. Funct. Mater.* **2009**, *19*, 2782–2789.
15. Rao, C. N. R.; Sood, A. K.; Voggu, R.; Subrahmanyam, K. S. Some Novel Attributes of Graphene. *J. Phys. Chem. Lett.* **2010**, *1*, 572–580.
16. Wang, G. X.; Shen, X. P.; Wang, B.; Yao, J.; Park, J. Synthesis and Characterization of Hydrophilic and Organophilic Graphene Nanosheets. *Carbon* **2009**, *47*, 1359–1364.
17. Si, Y.; Samulski, E. T. Synthesis of Water Soluble Graphene. *Nano Lett.* **2008**, *8*, 1679–1682.
18. Niyogi, S.; Bekyarova, E.; Itkis, M. E.; McWilliams, J. L.; Hamon, M. A.; Haddon, R. C. Solution Properties of Graphite and Graphene. *J. Am. Chem. Soc.* **2006**, *128*, 7720–7721.
19. Verdejo, R.; Barroso-Bujans, F.; Rodriguez-Perez, M. A.; Saja, J. A. D.; Lopez-Manchado, M. A. Functionalized Graphene Sheet Filled Silicone Foam Nanocomposites. *J. Mater. Chem.* **2008**, *18*, 2221–2226.
20. Stankovich, S.; Dikin, D. A.; Dommett, G. H. B.; Kohlhaas, K. M.; Zimney, E. J.; Stach, E. A.; Piner, R. D.; Nguyen, S. T.; Ruoff, R. S. Graphene-Based Composite Materials. *Nature* **2006**, *442*, 282–286.
21. Stankovich, S.; Piner, R. D.; Chen, X.; Wu, N.; Nguyen, S. T.; Ruoff, R. S. Stable Aqueous Dispersions of Graphitic Nanoplatelets *via* the Reduction of Exfoliated Graphite Oxide in the Presence of Poly(Sodium 4-styrenesulfonate). *J. Mater. Chem.* **2006**, *16*, 155–158.
22. Liu, N.; Luo, F.; Wu, H.; Liu, Y.; Zhang, C.; Chen, J. One-Step Ionic-Liquid-Assisted Electrochemical Synthesis of Ionic-Liquid-Functionalized Graphene Sheets Directly from Graphite. *J. Adv. Funct. Mater.* **2008**, *18*, 1518–1525.
23. Patil, A. J.; Vickery, J. L.; Scott, T. B.; Mann, S. Aqueous Stabilization and Self-Assembly of Graphene Sheets into Layered Bio-nanocomposites Using DNA. *Adv. Mater.* **2009**, *21*, 3159–3164.
24. Su, Q.; Pang, S. P.; Alijani, V.; Li, C.; Feng, X. L.; Müllen, K. Composites of Graphene with Large Aromatic Molecules. *Adv. Mater.* **2009**, *21*, 3191–3195.
25. Liang, Y. Y.; Wu, D. Q.; Feng, X. L.; Müllen, K. Dispersion of Graphene Sheets in Organic Solvent Supported by Ionic Interactions. *Adv. Mater.* **2009**, *21*, 1679–1683.
26. Si, Y. C.; Samulski, E. T. Synthesis of Water Soluble Graphene. *Nano Lett.* **2008**, *8*, 1679–1682.
27. Rekharsky, M.; Inoue, Y. Complexation Thermodynamics of Cyclodextrins. *Chem. Rev.* **1998**, *98*, 1875–1918.
28. Wang, F.; Khaledi, M. G. Chiral Separations by Nonaqueous Capillary Electrophoresis. *Anal. Chem.* **1996**, *68*, 3460–3467.
29. Freeman, R.; Finder, T.; Bahshi, L.; Willner, I. β-Cyclodextrin-Modified CdSe/ZnS Quantum Dots for Sensing and Chiroselective Analysis. *Nano Lett.* **2009**, *9*, 2073–2076.
30. Onclin, S.; Huskens, J.; Ravoo, B. J.; Reinhouldt, D. N. Molecular Boxes on a Molecular Printboard: Encapsulation of Anionic Dyes in Immobilized Dendrimers. *Small* **2005**, *1*, 852–857.
31. Ang, P. K.; Wang, S.; Bao, Q.; Thong, J. T. L.; Loh, K. P. High-Throughput Synthesis of Graphene by Intercalation−Exfoliation of Graphite Oxide and Study of Ionic Screening in Graphene Transistor. *ACS Nano* **2009**, *3*, 3587–3594.
32. Li, D.; Muller, M. B.; Gilje, S.; Kaner, R. B.; Wallace, G. G. Processable Aqueous Dispersions of Graphene Nanosheets. *Nat. Nanotechnol.* **2008**, *3*, 101.
33. Scatena, L. F.; Brown, M. G.; Richmond, G. L. Water at Hydrophobic Surfaces: Weak Hydrogen Bonding and Strong Orientation Effects. *Science* **2001**, *292*, 908–912.

34. Stockton, W. B.; Rubner, M. F. Molecular-Level Processing of Conjugated Polymers. 4. Layer-by-Layer Manipulation of Polyaniline *via* Hydrogen-Bonding Interactions. *Macromolecules* **1997**, *30*, 2717–2725.
35. Wang, L. Y.; Wang, Z. Q.; Zhang, X.; Shen, J. C.; Chi, L. F.; Fuchs, H. A new approach for the fabrication of an alternating multilayer film of poly(4-vinylpyridine) and poly(acrylic acid) based on hydrogen bonding. *Macromol. Rapid Commun.* **1997**, *18*, 509–514.
36. Wang, L. Y.; Cui, S. X.; Wang, Z. Q.; Zhang, X.; Jiang, M.; Chi, L. F.; Fuchs, H. Multilayer Assemblies of Copolymer PSOH and PVP on the Basis of Hydrogen Bonding. *Langmuir* **2000**, *16*, 10490–10494.
37. Zhang, H. Y.; Fu, Y.; Wang, D.; Wang, L. Y.; Wang, Z. Q.; Zhang, X. Hydrogen-Bonding-Directed Layer-by-Layer Assembly of Dendrimer and Poly(4-vinylpyridine) and Micropore Formation by Post-Base Treatment. *Langmuir* **2003**, *19*, 8497–8502.
38. Bai, H.; Xu, Y.; Zhao, L.; Li, C.; Shi, G. Noncovalent Functionalization of Graphene Sheets by Sulfonated Polyaniline. *Chem. Commun.* **2009**, 1667–1669.
39. Xu, Y.; Bai, H.; Lu, G.; Li, C.; Shi, G. Flexible Graphene Films *via* the Filtration of Water-Soluble Noncovalent Functionalized Graphene Sheets. *J. Am. Chem. Soc.* **2008**, *130*, 5856–5857.
40. Zhu, C.; Guo, S.; Fang, Y.; Dong, S. Reducing Sugar: New Functional Molecules for the Green Synthesis of Graphene Nanosheets. *ACS Nano* **2010**, *4*, 2429–2437.
41. Guo, H. L.; Wang, X. F.; Qian, Q. Y.; Wang, F. B.; Xia, X. H. A Green Approach to the Synthesis of Graphene Nanosheets. *ACS Nano* **2009**, *3*, 2653–2659.
42. Stankovich, S.; Dikin, D. A.; Piner, R. D.; Kohlhaas, K. A.; Kleinhammes, A.; Jia, Y.; Wu, Y.; Nguyen, S. T.; Ruoff, R. S. Synthesis of Graphene-Based Nanosheets *via* Chemical Reduction of Exfoliated Graphite Oxide. *Carbon* **2007**, *45*, 1558–1565.
43. Alarcon-Angeles, G.; Perez-Lopez, B.; Palomar-Pardave, M.; Ramirez-Silva, M. T.; Alegret, S.; Merkoci, A. Enhanced Host−Guest Electrochemical Recognition of Dopamine Using Cyclodextrin in the Presence of Carbon Nanotubes. *Carbon* **2008**, *46*, 898–906.
44. Li, M. Q.; Jing, L. H. Electrochemical Behavior of Acetaminophen and Its Detection on the PANI-MWCNTs Composite Modified Electrode. *Electrochim. Acta* **2007**, *52*, 3250–3257.
45. Zhou, M.; Zhai, Y. M.; Dong, S. J. Electrochemical Sensing and Biosensing Platform Based on Chemically Reduced Graphene Oxide. *Anal. Chem.* **2009**, *81*, 5603–5613.
46. Chen, P.-Y.; Vittal, R.; Nien, P.-C.; Ho, K.-C. Enhancing Dopamine Detection Using a Glassy Carbon Electrode Modified with MWCNTs, Quercetin, and Nafion. *Biosens. Bioelectron.* **2009**, *24*, 3504–3509.
47. He, J.-L.; Yang, Y.; Yang, X.; Liu, Y.-L.; Liu, Z.-H.; Shen, G.-L.; Yu, R.-Q. Beta-Cyclodextrin Incorporated Carbon Nanotube-Modified Electrode As an Electrochemical Sensor for Rutin. *Sens. Actuators B* **2006**, *114*, 94–100.
48. Hummers, W.; Offeman, R. J. Preparation of Graphitic Oxide. *J. Am. Chem. Soc.* **1958**, *80*, 1339.
49. Kovtyukhova, N. I.; Ollivier, P. J.; Martin, B. R.; Mallouk, T. E.; Chizhik, S. A.; Buzaneva, E. V.; Gorchinskiy, A. D. Layer-by-Layer Assembly of Ultrathin Composite Films from Micron-Sized Graphite Oxide Sheets and Polycations. *Chem. Mater.* **1999**, *11*, 771–778.